Salvia Miltiorrhiza Extract Prevents Atherosclerosis Development via TLR4/ NF-κB Pathway

Jiangli Wang
Hebei University of Chinese Medicine
Hongjun Xu
Hebei University of Chinese Medicine
Wei Zhao
Hebei University of Chinese Medicine
Qingzhuo Cui
Hebei University of Chinese Medicine
Luyang Zhou
Hebei University of Chinese Medicine
Yongjie Zhou
Hebei University of Chinese Medicine
Shengjun An (sjsjan@126.com)
Hebei University of Chinese Medicine https://orcid.org/0000-0001-8765-0396

Research Article

Keywords: Salvia miltiorrhiza, TLR4/ NF-κB pathway, Atherosclerosis, ApoE-/- mice.

Posted Date: February 19th, 2021

DOI: https://doi.org/10.21203/rs.3.rs-214790/v1

Salvia Miltiorrhiza extract prevents atherosclerosis development via TLR4/ NF-κB pathway

Jiangli Wu[1,2*], Hongjun Xu[2,3*], Wei Zhao[2,3,4], Qingzhuo Cui[2,3], Luyang Zhou[2,3], Yongjie Zhou[2,3] , Shengjun An[1,2,3]

[1]Scientific Research Center, Hebei University of Chinese Medicine, Shijiazhuang/050200, China.

[2]Hebei Provincial Engineering Laboratory of Plant Bioreactor Preparation Technology, Shijiazhuang/050200, China.

[3] College of integrated Chinese and western medicine, Hebei University of Chinese Medicine, Shijiazhuang/050200, China.

4 Affiliated Hospital of Hebei University of Engineering, Handan/056000, China.

*These authors contribute equally to this study.

Running Title: Chinese medicine and atherosclerosis

Correspondence should be addressed to

Dr. Shengjun An, MD, PhD, Hebei Engineering Center of Plant Bioreactor Preparation Technology, Hebei University of Chinese Medicine. No. 326 Xinshi south Road, Qiaoxi District, Shijiazhuang 050090 Hebei, China E-mail: sjsjan@126.com

Word Count: Total: 4510; Abstract: 291; Introduction: 420; Results: 496; Discussion: 753.

Abstract

Aim of the Study

Aqueous extract from Salvia Miltiorrhiza has been traditionally used to treat cardiovasulcar diseases. This study aims to explore the anti-inflammatory mechanisms underlying attenuation of atherosclerosis development by aqueous extract from Salvia Miltiorrhiza.

Materials and methods

Male ApoE$^{-/-}$ mice were randomly allocated into the model, the SABP, and the rosuvastatin calcium groups (RC). After 8-wk-treatment, the lipid profiles in serum, the lactate dehydrogenase (LDH), and creatine kinase (CK) in heart tissue were measured and the morphology alterations of thoracic aorta and heart were assessed. The protein expression of Toll-like receptor 4 (TLR4), TGF beta-activated kinase 1 (TAK1), nuclear factor kappa-B (NF-κB), interleukin-6 (IL-6) and tumor necrosis factor-α (TNF-α) in the heart tissue were determined by western blotting analysis. The serum low-density lipoprotein cholesterol (LDL-C), triglyceride (TG), and total cholesterol (TC) levels were increased and the high-density lipoprotein cholesterol (HDL-C) level was decreased in ApoE$^{-/-}$ mice.

Results

SABP significantly decreased the serum lipid levels and improved histopathology in the thoracic aorta. In addition, SABP treatment reduced the expression of TLR4, TAK1, NF-κB, IL-6, and TNF-α, and inhibited the expression and activation of NF-κB in the heart of ApoE$^{-/-}$ mice. The LDH and CK in the heart did not differ significantly among different groups, and the heart did not have obvious pathological changes.

Conclusions

These findings indicated that SABP may exert an anti-atherosclerotic effect by lowering blood lipids and inhibiting inflammatory response via TLR4/ NF-κB signaling pathway.

Keywords: Salvia miltiorrhiza, TLR4/ NF-κB pathway, Atherosclerosis, ApoE$^{-/-}$ mice.

List of Abbreviations:

SM: Salvia Miltiorrhiza; **TLR4**: Toll-like receptor 4; **TAK1**: TGF beta-activated kinase 1; **NF-κB**: nuclear factor kappa-B; **IL-6**: interleukin-6; **TNF-α**: tumor necrosis factor-α; **LDH** lactate dehydrogenase; **CK**: creatine kinase; **LDL-C**: low-density lipoprotein cholesterol; **TG**: triglyceride; **TC**: total cholesterol; **HDL-C**: high-density lipoprotein cholesterol; **ApoE**: apoliprotein E.

Introduction

Atherosclerosis (AS) may induce fatal cardiovascular conditions involving the aorta and coronary arteries. Although several mechanisms such as thrombogenic theory, lipid infiltration theory, oxidative hypothesis, and smooth muscle mutation theory have been proposed to be involved in the pathogenesis of the AS, it is now widely accepted that inflammation plays an important role in the pathological processing of AS (Greaves and Channon, 2002; Libby, 2002). Toll-like receptor 4 (TLR4)/nuclear factor kappa-B (NF-κB) signaling pathway is involved in the initiation and subsequent progression of AS by regulating the secretion of inflammatory factors (Bowman et al., 2017; Cole et al., 2010; den Dekker et al., 2010; Xing et al., 2014). Therefore, regulating the key molecules involved in the inflammatory signaling pathway becomes a new approach to prevent and treat the AS. In addition, PPARγ, mitogen-activated protein kinase (Jang et al., 2006), and Jak/STAT3 are also involved in the anti-AS mechanism (Nizamutdinova et al., 2012). It has been reported that high levels of HDL are protective against the progression and complications of the AS (Cockerill et al., 2001).

Salvia miltiorrhiza (SM) is the root of *Salvia miltiorrhiza* of Labiatae, the major component of "decoction of Four Drugs", which were documented in the ancient books of traditional chinese medicine. It has been widely used clinically with a remarkable beneficiary effect on cardiovascular and cerebrovascular diseases (Su et al., 2016). Because decoction is the traditional model of using SM, the active ingredients can be dissolved aqueously. Studies on aqueous extracts from the SM have shown many new findings. For example, salvianolic acid A (Sal-A) attenuates aortic aneurysm formation in apoliprotein E(ApoE)-deficient mice (Zhang et al., 2014). Salvianolic acid B (Sal-B) exerted anti-liver fibrosis effects (Wu et al., 2019) and anti-inflammatory properties (Bao et al., 2012). Both Danshensu (DSS) and Sal-A prevent myocardium remodeling in spontaneously hypertensive rats (Jiang et al., 2013; Tang et al., 2011). Protocatechuic aldehyde (PAL) protects the cardiovascular system against inflammation and AS (Fang et al., 2018). A combination effective components from Chinese herbal medicine is the new model of Chinese herbal medicine compatibility. SM has four major aqueous extract components: DSS, Sal-A, Sal-B, and PAL, named as SABP (Zhou et al., 2016). The monomer component of traditional Chinese medicine is a current research

focus (Lin et al., 2016) and maybe a potential alternative medicine from SM.

Our laboratory has found that SABP reduces blood pressure (Zhang et al., 2016). However, the effect of SABP on AS has not been reported. Previous studies mainly focus on the stenosis of vessel lesion caused by the AS. This study aims at investigating whether SABP exerts anti-inflammatory roles in protecting the heart in $ApoE^{-/-}$ mice via the TLR4/NF-κB signaling pathway. Our data provided new insights into the mechanism of pathogenesis of inflammation-associated diseases, and the mechanistic basis for the use of SABP as a therapeutic approach against inflammation-associated diseases.

Materials and Methods

Chemicals and reagents

Injectable solutions of DSS (76822-21-4), Sal-A (96574-01-5), Sal-B (115939-25-8), and PAL (139-85-5) was purchased respectively from Shanghai Fu Life Industry Co. Ltd., China. TLR4 antibody (JL-20594R) was obtained from Shanghai Jianglai Science and Technology Ltd. Antibodies against NF-KB p65 (GB11142), IL-6 (GB11117), TAK1 (GB11701), TNF-α (GTX110520), and H3 (GB13102-1) were purchased from Wuhan Seville Technology Co., Ltd., GAPDH antibody (AC033) were purchased from AB clonal company. Sheep anti-rabbit secondary antibody, sheep anti-mouse secondary antibody was purchased from KPL company. Nuclear and Cytoplasmic Protein Extraction Kit (P0027) was purchased from Beyotime Biotechnology Co., Ltd.

Experimental animals and treatment

Thirty male ApoE$^{-/-}$ mice and ten C57BL/6J mice (6 weeks of age, 18-22 g) were purchased from Beijing Vital River Laboratory Animal Technology Co., Ltd. (Certificate number SCXK (Beijing): 2016-0010). Mice were housed in a climate-controlled environment (12 h light-dark cycle at 22℃) and fed with standard diet and water ad libitum. After one week of acclimatization, all ApoE$^{-/-}$ mice (n = 30) were randomly assigned into 3 groups: the ApoE$^{-/-}$ (model) group, the SABP group, the rosuvastatin calcium (RC) group. The C57BL/6 mice were defined as the normal control group. The RC group received daily intraperitoneal (i.p.) injection of RC (0.4 mg/kg/d). The SABP group received daily i.p. injection of SABP (DSS: 5 mg/kg/d, Sal-A: 0.233 mg/kg/d, Sal-B: 10 mg/kg/d, PAL: 17 mg/kg/day)[19] in which uniform and orthogonal design formulas were applied to divide into groups and composition. Drugs were dissolved in normal saline. The ApoE$^{-/-}$ model and C57BL/6 mice received daily i.p. injection of an equal volume of saline. After 8 weeks of treatment, the mice were anaesthetized with 2% isoflurane. The tissues were harvested, then the thoracic aorta and heart were fixed in 4% formalin for histopathological study and the remaining portion was stored at −80℃ for biochemical study. All procedures were approved by the Animal Care and Use Committee of Medical Ethics of the Hebei University of Chinese Medicine.

Measurement of serum lipid profiles

Blood samples from the above 4 groups of mice were collected and then centrifuged at 3500 g for 15 min at 4℃. The supernatants were collected and stored at −80℃ until use. The levels of total cholesterol (TC), triglyceride (TG), high-density lipoprotein-cholesterol (HDL-C) and low-density lipoprotein-cholesterol (LDL-C) were measured using an automatic biochemical analyzer (iCubio Biomedical Technology Co., Ltd, Shenzhen, China).

Cardiac function index

The lactate dehydrogenase (LDH) and creatine kinase (CK) levels were determined in the heart homogenate by an automatic biochemical analyzer (iCubio Biomedical Technology Co., Ltd, Shenzhen, China).

Histopathological study

The heart and aorta were removed and soaked into 4% polyformaldehyde. After a gradient alcohol dehydration, xylene was transparent, the paraffin was embedded. The tissues were sectioned at a thickness of 6 μm. Hematoxylin and Eosin (H&E) staining were performed to observe the pathological changes of the heart and aorta.

Immunohistochemistry staining

After deparaffinization of paraffin sections, rehydration was done and the endogenous peroxidase was blocked by 3% H_2O_2. Then， the sections were incubated with normal goat serum at 37℃ for 20 min and subsequently incubated with rabbit polyclonal antibodies against TLR4 (1:500), NF-κB (1:200), IL-6 (1:400) and TNF-α (1:500) at 4℃ overnight. After being rinsed, the sections were incubated with a horseradish peroxidase (HRP)-labeled secondary goat anti-rabbit antibody for 30 min. Antigens were visualized with the diaminobenzidine (DAB) approach. Immunostained paraffin sections were photographed under a light microscope (Leica, Germany) and a proportion of positive immunostained sections were analyzed using Image-Pro Plus 6.0.

Western Blotting

The heart tissues were homogenized and the lysates were collected to obtain the total protein using lysis buffer (Beijing Solarbio Science and Technology Co., Ltd., Beijing, China). Nuclear proteins were extracted using nuclear and cytoplasmic protein extraction kit (Beyotime Biotechnology Co., Ltd., Beijing, China), according to the manufacturer's protocol. Total protein and nuclear protein were extracted and their concentrations in all

samples were quantified with the bicinchoninic acid (BCA) protein assay (Applygen Technologies Inc., Beijing, China). Subsequently, proteins were separated on 10% SDS-PAGE gel and transferred to a PVDF membrane. After blocking in 5% skimmed milk for 2 h, the membranes were incubated with primary antibodies against TLR4 (1:1000), NF-κB (1:1000), IL-6 (1:1000), TAK-1 (1:750), GAPDH (1:10000), and H3 (1:10000). Then the membranes were incubated with an HRP-conjugated secondary antibody followed by ECL detection (Vilber Fusion FX5 Spectra, Paris, France). And the bands were analyzed semi-quantitatively with Image J software (National Institutes of Health, Bethesda, Maryland, USA).

Statistical analysis

All the data were expressed as mean ± standard deviation (SD). SPSS 19.0 software was used for one-way analysis of variance (ANOVA) and *post hoc* repeated measurement. A value of $P < 0.05$ was considered statistically significant.

Results

Effect of SABP on lipid levels in serum

ApoE$^{-/-}$ mice showed higher levels of TC, TG and LDL-C and a lower level of HDL-C in the model group than mice in the control group. SABP treatment decreased the serum TG, TC and LDL-C levels in ApoE$^{-/-}$ mice ($P<0.05$) (Figure 1). SABP treatment slightly increased HDL-C level was ApoE$^{-/-}$ mice ($P>0.05$). However, there were no differences in serum TC, TG, LDL-C, and HDL-C levels between the model group and those treated with RC. These data indicated that SABP treatment dramatically altered the serum lipid profile in normal diet-fed ApoE$^{-/-}$ mice.

Effect of SABP on LDH and CK levels in the heart

However, we found that the LDH and CK in heart tissues did not differ in control, ApoE$^{-/-}$ mice, SABP-treated ApoE$^{-/-}$ mice (Figure 2), suggesting that the cardiac function did not alter in ApoE$^{-/-}$ mice.

The thoracic aorta and cardiac histological changes

In the control group, the three layers of the aorta were clear, the intimal surface was covered with monolayer flat endothelial cells. The tunica media was composed of smooth muscle cells with a neat arrangement. The outer membrane was intact and the inner wall of the official cavity was smooth. No abnormal substance proliferation was found. In the model group, the vascular wall structure was disordered and the intima was seriously injured and thickened. The arrangement of smooth muscle cells in the middle layer was disordered. No AS plaques were found in the official cavity. In the RC and SABP group, the vascular endothelial cells had no obvious morphological changes and the smooth muscle cells of the tunica media were arranged neatly (Figure 3A). The thickness of both adventitia and intima was increased in the model group compared with the control group and the RC and SABP groups ($P<0.05$) (Figure 3B, D). The thickness of tunica media did not have any obvious changes among the groups ($P>0.05$) (Figure 3C).

The myocardial fibers in the model and the other three groups were arranged neatly, the cell nucleus of the cardiac myocyte was located in the center of the cells and shaped in oval or round. No thickening, no congestion, hemorrhage, and other lesions were found in the myocardial fibers (Figure 4).

SABP regulated expression of the TLR4/NF-κB signal pathway in the heart

To elucidate the molecular mechanism underlying SABP anti-inflammation effect, we evaluated the expression of TLR4, TAK1, activated NF-κB, IL-6, and TNF-α in the heart by immunohistochemistry staining and western blotting analysis. Immunohistochemistry staining and Western blotting analysis indicated that the expression of TLR4, IL-6, TNF-α, and TAK1 proteins were upregulated and NF-κB was activated in the heart tissue of $ApoE^{-/-}$ mice in the model group (Figures 5 and 6). Compared with $ApoE^{-/-}$ mice in the model group, TLR4, TAK1, IL-6, and TNF-α protein were significantly decreased, and activated NF-κB was inhibited in SABP group ($P < 0.05$). These data indicated that SABP treatment regulated the AS by affecting the TLR4/NF-κB pathway and associated proteins.

Discussion

This study demonstrated that a mixture of aqueous extract of SM SABP exerts an anti-atherosclerotic effect at all combinations of four aqueous components in formulas designated uniform and orthogonal approaches. Salvia miltiorrhiza is a chinese herbal medicine (CHM) for improving cardiovascular function. Studies have shown that hydrophilic phenolic acids derived from SM are the active ingredients. SABP is the effective aqueous extracts of SM and it performs a new model of chinese herbal medicine compatibility. This mixture of the four monomers might contribute to anti-atherosclerotic effects from the medicinal herbs.

In this study, AS was detected in ApoE$^{-/-}$ mice fed with a common diet for 8 weeks. Expression levels of inflammatory proteins and factors involved in TLR4/NF-κB signal pathway were increased in the ApoE$^{-/-}$ mice group compared with the C57BL/6 mice group. These data suggested that SABP treatment could attenuate AS by reducing the inflammatory response. ApoE$^{-/-}$ mice could form hyperlipidemia and further form plaques, regardless of whether they were fed with a basic or high-fat diet. In this study, after 8 weeks of feeding with a common diet, serum TC, TG, and LDL-C in the model group were increased significantly and HDL-C was significantly decreased. These findings suggest that ApoE$^{-/-}$ mice had serious hyperlipidemia. However, no plaques were found in the HE staining of the thoracic aorta. It is likely that 8-week normal diet feeding in 6-week old ApoE$^{-/-}$ mice was not enough to form lipid plaque. Studies have reported that AS plaque was formed after 6-week-old ApoE$^{-/-}$ mice fed with a high-fat diet for 13 weeks (Chen et al., 2019). Additionally, the cardiac function indexes and the pathology results all indicated that ApoE$^{-/-}$ mice heart did not have obvious pathological changes. Statins are widely used in the prevention and treatment of AS, because of their protective effects on vascular endothelial cells, anti-inflammation, and lipid-lowering (Shapiro and Fazio, 2016; Zhou and Liao, 2010). However, it has been shown that statins are not able to reduce cholesterol in ApoE$^{-/-}$ mice because of the lack of critical ligands for LDL receptor (ApoE), which is important for lowing cholesterol (Zadelaar et al., 2007; Zhou and Liao, 2010). This notion has been supported by studies done by Song Ke and Yang (Yang et al., 2013). The results of this study are consistent with the findings from previous studies that statins cannot reduce the level of

blood lipids in ApoE$^{-/-}$ mice. However, whether SABP has effects on serum levels of lipids is still not clear. In this study, we demonstrated that SABP treatment lowered TC, TG, and LDL-C. Although lipid metabolism is importantly linked to the AS, reducing blood lipids alone does not account for the mechanism underlying the ability of SABP in the prevention and treatment of the AS.

The TLR4 signal pathway is associated with inflammation in many disease conditions such as colitis (Feng et al., 2014), and intracerebral hemorrhage (Fei et al., 2019). Growing evidence suggests that the TLR4 signal pathway is involved in inflammation during development of AS (Ha et al., 2018; Shinohara et al., 2007). The TLR4-triggered intracellular signal pathway recruits downstream proteins and finally activate NF-κB, which leads to the release of NF-κB and nuclear translocation, followed by upregulating the expression of inflammatory mediators including IL-6 and TNF-α (Baeuerle and Baltimore, 1988; Bohannon et al., 2013; Ha et al., 2018). Our results revealed that SABP reduced the expression of TLR4 and TAK1. Thus, we hypothesized that the anti-inflammation mechanism of SABP is related to TLR4 signals. We also determined the protein levels of NF-κB in the nucleus and found that SABP inhibited NF-κB activation. We further examined the expression of inflammatory factors IL-6 and TNF-α. We found that SABP could profoundly inhibit the expression of these inflammation-related molecules. These findings suggest that SABP suppresses the AS by inhibition of the TLR4/NF-κB signaling pathway, accompanied by repression of inflammatory factors.

We showed, for the first time, that SABP played an important role in attenuating AS through downregulation of the expression of key protein involved in the TLR4/NF-κB pathway. The present study revealed that SABP inhibited AS-related inflammation, partly through inhibition of the TLR4/NF-κB activity. If further study is needed, it is necessary to block this pathway in the subsequent in vitro experiments to identify the specific components in the signaling pathways involved in the effect of SABP.

Conclusion This study is the first to demonstrate that SABP is able to alleviate the development of AS. The underlying mechanisms involved in the action of SABP on AS were improving blood lipids metabolism and inhibiting the TLR4/NF-κB signaling pathway. These findings indicate that the efficacy and function from the optimal compatibility ratio of SM

active ingredients represents a new strategy to treat atherosclerosis by the SM.

Author contributions

Conceived and designed the experiments: Wu J., Xu H., and An S.. Performed the experiments: and Zhou L.. Contributed reagents/materials/analytical tools: Zhao W., Cui Q., and Zhou L.. Analyzed the data: Wu J., Xu H., Zhao W., Cui Q., Zhou Y., and An S.. Wrote and revised the paper: Wu J., Xu H., and An S..

Declaration of competing interest

All authors have declared no conflict of interest.

Acknowledgement:

The authors acknowledge the following sponsors to provide financial support for this study National Natural Science Foundation of China (grant no.81873230), Research Project of Hebei Traditional Chinese Medicine Administration (2019073) and Science and Technology Capability Improvement Project of Hebei University of Chinese Medicine (KTZ2019016).

Data Availability

The data used to support the findings of this study are included in the article.

References:

Baeuerle, P.A., Baltimore, D., 1988. I kappa B: a specific inhibitor of the NF-kappa B transcription factor. Science 242(4878), 540-546.

Bao, Y., Wang, L., Xu, Y., Yang, Y., Wang, L., Si, S., Cho, S., Hong, B., 2012. Salvianolic acid B inhibits macrophage uptake of modified low density lipoprotein (mLDL) in a scavenger receptor CD36-dependent manner. Atherosclerosis 223(1), 152-159.

Bohannon, J.K., Hernandez, A., Enkhbaatar, P., Adams, W.L., Sherwood, E.R., 2013. The immunobiology of toll-like receptor 4 agonists: from endotoxin tolerance to immunoadjuvants. Shock 40(6), 451-462.

Bowman, J.D., Surani, S., Horseman, M.A., 2017. Endotoxin, Toll-like Receptor-4, and Atherosclerotic Heart Disease. Curr Cardiol Rev 13(2), 86-93.

Chen, Z., Gao, X., Jiao, Y., Qiu, Y., Wang, A., Yu, M., Che, F., Li, S., Liu, J., Li, J., Zhang, H., Yu, C., Li, G., Gao, Y., Pan, L., Sun, W., Guo, J., Cao, B., Zhu, Y., Xu, H., 2019. Tanshinone IIA Exerts Anti-Inflammatory and Immune-Regulating Effects on Vulnerable Atherosclerotic Plaque Partially via the TLR4/MyD88/NF-kappaB Signal Pathway. Front Pharmacol 10, 850.

Cockerill, G.W., Huehns, T.Y., Weerasinghe, A., Stocker, C., Lerch, P.G., Miller, N.E., Haskard, D.O., 2001. Elevation of plasma high-density lipoprotein concentration reduces interleukin-1-induced expression of E-selectin in an in vivo model of acute inflammation. Circulation 103(1), 108-112.

Cole, J.E., Georgiou, E., Monaco, C., 2010. The expression and functions of toll-like receptors in atherosclerosis. Mediators Inflamm 2010, 393946.

den Dekker, W.K., Cheng, C., Pasterkamp, G., Duckers, H.J., 2010. Toll like receptor 4 in atherosclerosis and plaque destabilization. Atherosclerosis 209(2), 314-320.

Fang, X., Liu, Y., Lu, J., Hong, H., Yuan, J., Zhang, Y., Wang, P., Liu, P., Ye, J., 2018. Protocatechuic aldehyde protects against isoproterenol-induced cardiac hypertrophy via inhibition of the JAK2/STAT3 signaling pathway. Naunyn Schmiedebergs Arch Pharmacol 391(12), 1373-1385.

Fei, X., Chen, C., Kai, S., Fu, X., Man, W., Ding, B., Wang, C., Xu, R., 2019. Eupatilin attenuates the inflammatory response induced by intracerebral hemorrhage through the

TLR4/MyD88 pathway. Int Immunopharmacol 76, 105837.
Feng, J., Guo, C., Zhu, Y., Pang, L., Yang, Z., Zou, Y., Zheng, X., 2014. Baicalin down regulates the expression of TLR4 and NFkB-p65 in colon tissue in mice with colitis induced by dextran sulfate sodium. Int J Clin Exp Med 7(11), 4063-4072.
Greaves, D.R., Channon, K.M., 2002. Inflammation and immune responses in atherosclerosis. Trends Immunol 23(11), 535-541.
Ha, S.J., Lee, J., Song, K.M., Kim, Y.H., Lee, N.H., Kim, Y.E., Jung, S.K., 2018. Ultrasonicated Lespedeza cuneata extract prevents TNF-alpha-induced early atherosclerosis in vitro and in vivo. Food Funct 9(4), 2090-2101.
Jang, S.I., Kim, H.J., Kim, Y.J., Jeong, S.I., You, Y.O., 2006. Tanshinone IIA inhibits LPS-induced NF-kappaB activation in RAW 264.7 cells: possible involvement of the NIK-IKK, ERK1/2, p38 and JNK pathways. Eur J Pharmacol 542(1-3), 1-7.
Jiang, B., Li, D., Deng, Y., Teng, F., Chen, J., Xue, S., Kong, X., Luo, C., Shen, X., Jiang, H., Xu, F., Yang, W., Yin, J., Wang, Y., Chen, H., Wu, W., Liu, X., Guo, D.A., 2013. Salvianolic acid A, a novel matrix metalloproteinase-9 inhibitor, prevents cardiac remodeling in spontaneously hypertensive rats. PLoS One 8(3), e59621.
Libby, P., 2002. Inflammation in atherosclerosis. Nature 420(6917), 868-874.
Lin, C., Liu, Z., Lu, Y., Yao, Y., Zhang, Y., Ma, Z., Kuai, M., Sun, X., Sun, S., Jing, Y., Yu, L., Li, Y., Zhang, Q., Bian, H., 2016. Cardioprotective effect of Salvianolic acid B on acute myocardial infarction by promoting autophagy and neovascularization and inhibiting apoptosis. J Pharm Pharmacol 68(7), 941-952.
Nizamutdinova, I.T., Kim, Y.M., Jin, H., Son, K.H., Lee, J.H., Chang, K.C., Kim, H.J., 2012. Tanshinone IIA inhibits TNF-alpha-mediated induction of VCAM-1 but not ICAM-1 through the regulation of GATA-6 and IRF-1. Int Immunopharmacol 14(4), 650-657.
Shapiro, M.D., Fazio, S., 2016. From Lipids to Inflammation: New Approaches to Reducing Atherosclerotic Risk. Circ Res 118(4), 732-749.
Shinohara, M., Hirata, K., Yamashita, T., Takaya, T., Sasaki, N., Shiraki, R., Ueyama, T., Emoto, N., Inoue, N., Yokoyama, M., Kawashima, S., 2007. Local overexpression of toll-like receptors at the vessel wall induces atherosclerotic lesion formation: synergism of TLR2 and TLR4. Arterioscler Thromb Vasc Biol 27(11), 2384-2391.

Su, P., Tong, Y., Cheng, Q., Hu, Y., Zhang, M., Yang, J., Teng, Z., Gao, W., Huang, L., 2016. Functional characterization of ent-copalyl diphosphate synthase, kaurene synthase and kaurene oxidase in the Salvia miltiorrhiza gibberellin biosynthetic pathway. Sci Rep 6, 23057.

Tang, Y., Wang, M., Chen, C., Le, X., Sun, S., Yin, Y., 2011. Cardiovascular protection with danshensu in spontaneously hypertensive rats. Biol Pharm Bull 34(10), 1596-1601.

Wu, C., Chen, W., Ding, H., Li, D., Wen, G., Zhang, C., Lu, W., Chen, M., Yang, Y., 2019. Salvianolic acid B exerts anti-liver fibrosis effects via inhibition of MAPK-mediated phospho-Smad2/3at linker regions in vivo and in vitro. Life Sci 239, 116881.

Xing, S., Zheng, F., Zhang, W., Wang, D., Xing, Q., 2014. Relationship between toll-like receptor 4 levels in aorta and severity of atherosclerosis. J Int Med Res 42(4), 958-965.

Yang, L.X., Heng, X.H., Guo, R.W., Si, Y.K., Qi, F., Zhou, X.B., 2013. Atorvastatin inhibits the 5-lipoxygenase pathway and expression of CCL3 to alleviate atherosclerotic lesions in atherosclerotic ApoE knockout mice. J Cardiovasc Pharmacol 62(2), 205-211.

Zadelaar, S., Kleemann, R., Verschuren, L., de Vries-Van der Weij, J., van der Hoorn, J., Princen, H.M., Kooistra, T., 2007. Mouse models for atherosclerosis and pharmaceutical modifiers. Arterioscler Thromb Vasc Biol 27(8), 1706-1721.

Zhang, J., An, S.J., Fu, J.Q., Liu, P., Shao, T.M., Li, M., Li, X., Jiao, Z., Chai, X.Q., 2016. Mixed Aqueous Extract of Salvia Miltiorrhiza Reduces Blood Pressure through Inhibition of Vascular Remodelling and Oxidative Stress in Spontaneously Hypertensive Rats. Cell Physiol Biochem 40(1-2), 347-360.

Zhang, T., Xu, J., Li, D., Chen, J., Shen, X., Xu, F., Teng, F., Deng, Y., Ma, H., Zhang, L., Zhang, G., Zhang, Z., Wu, W., Liu, X., Yang, M., Jiang, B., Guo, D., 2014. Salvianolic acid A, a matrix metalloproteinase-9 inhibitor of Salvia miltiorrhiza, attenuates aortic aneurysm formation in apolipoprotein E-deficient mice. Phytomedicine 21(10), 1137-1145.

Zhou, Q., Liao, J.K., 2010. Pleiotropic effects of statins. - Basic research and clinical perspectives. Circ J 74(5), 818-826.

Zhou, Y., Sun, W., Chen, J., Tan, H., Xiao, Y., Li, Q., Ji, Q., Gao, S., Chen, L., Chen, S., Zhang, L., Chen, W., 2016. SmMYC2a and SmMYC2b played similar but irreplaceable roles in regulating the biosynthesis of tanshinones and phenolic acids in Salvia miltiorrhiza. Sci

Rep 6, 22852.

Figure Legends:

Figure 1. TG, TC, LDL-C, and HDL-C serum lipid levels in response to SABP treatment. (A) The TG level; (B) The TC level; (C) The LDL-C level; (D) The HDL-C level. Data are presented as mean ± SEM. n=6 in each group. ＃P<0.05, compared with the control group; ＊P<0.05, compared with the model group.

Figure 2. The LDH and CK levels in the heart in response to SABP treatment. (A) The LDH level in the heart; (B) The CK level in the heart. Data are presented as mean ± SEM. n=6 rats in each group.

Figure 3. SABP attenuated the degree of AS-related lesion of the aorta in ApoE$^{-/-}$ mice. (A) HE staining of the aorta; (B) The adventitia thickness; (C) The tunica media thickness; (D) The intima thickness. Data are presented as mean ± SEM. n=6. ＃P<0.05, compared with the control group; ＊P<0.05, compared with the model group.

Figure 4. Observation of histologic changes of heart by HE staining.

Figure 5. SABP suppressed TLR4, NF-κB, IL-6, and TNF-α expression in the heart. (A-D) Normalized quantitative data for TLR4, NF-κB, IL-6, and TNF-α protein expression levels; (E) The TLR4, NF-κB, IL-6, and TNF-α expression were displayed by immunohistochemistry staining. The arrows showed the staining for targeted protein. Values are expressed as mean ± SEM, n=4. ＃P<0.05, compared with the control group; ＊P<0.05, compared with the model group.

Figure 6. SABP treatment regulated the TLR4, NF-κB, IL-6, and TAK1 expression in the heart. (A-D) Normalized quantitative data for TLR4, NF-κB, IL-6, and TAK1 protein expression. (E-F) Western blotting bands showed the TLR4, NF-κB, IL-6, and TAK1 protein expression levels. GAPDH was used as an internal control for normalization. Values are

expressed as mean ± SEM, n=4. # P<0.05, compared with the control group; * P<0.05, compared with the model group.

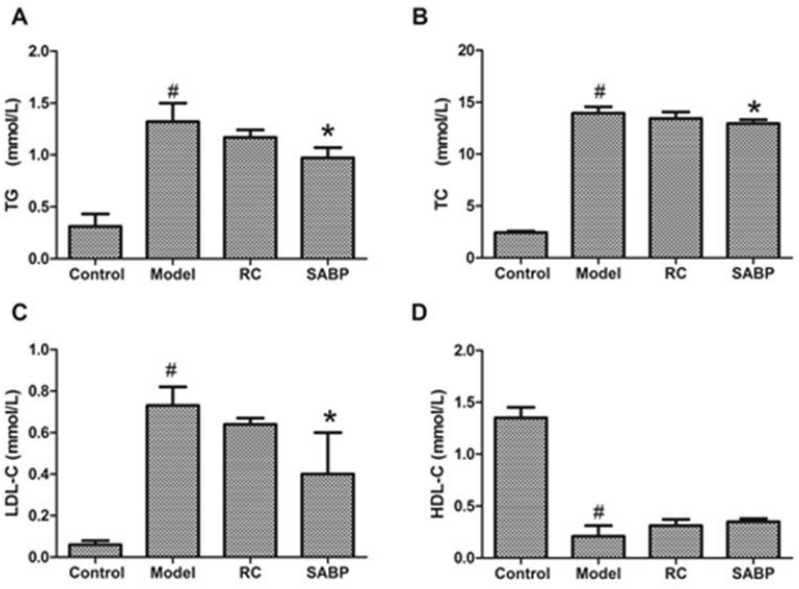
A
TG (mmol/L)
2.0
1.5
1.0
0.5
0.0
#
*
Control
Model
RC
SABP
B
TC (mmol/L)
20
15
10
5
0
#
*
Control
Model
RC
SABP
C
LDL-C (mmol/L)
1.0
0.8
0.6
0.4
0.2
0.0
#
*
Control
Model
RC
SABP
D
HDL-C (mmol/L)
2.0
1.5
1.0
0.5
0.0
#
Control
Model
RC
SABP

Figure 1

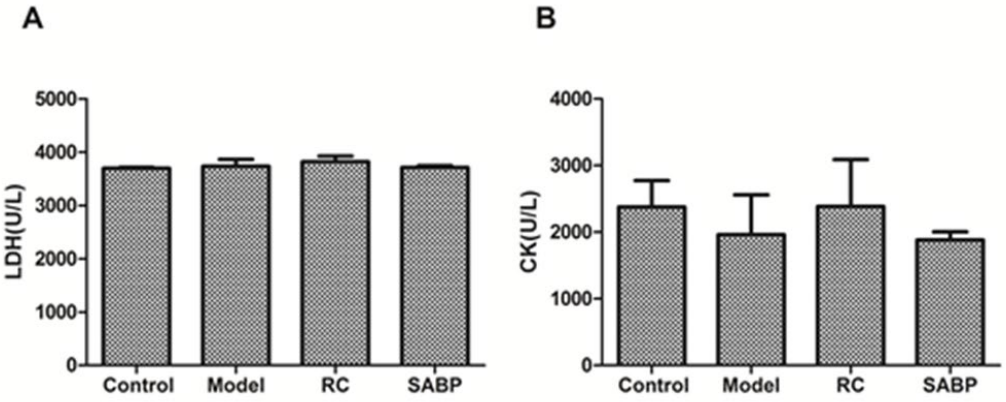
A
5000
4000
3000
2000
1000
0
LDH(U/L)
Control
Model
RC
SABP
B
4000
3000
2000
1000
0
CK(U/L)
Control
Model
RC
SABP

Figure 2

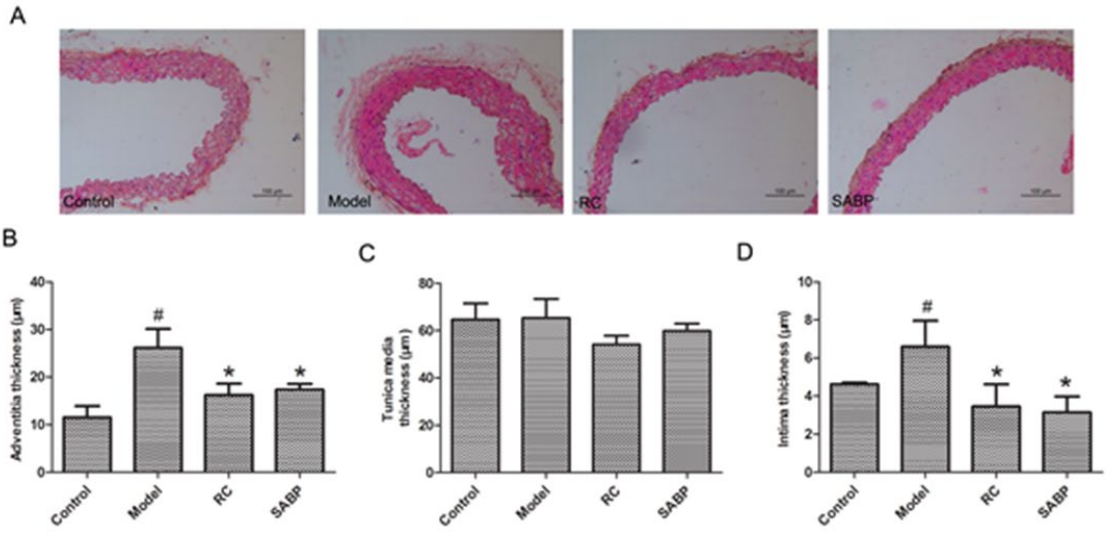
A
Control
Model
RC
SABP
B
Adventitia thickness (μm)
40
30
20
10
0
#
*
*
Control
Model
RC
SABP
C
Tunica media thickness (μm)
80
60
40
20
0
Control
Model
RC
SABP
D
Intima thickness (μm)
10
8
6
4
2
0
#
*
*
Control
Model
RC
SABP

Figure 3

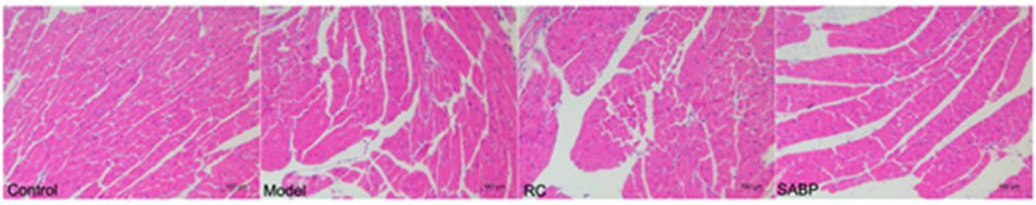

Figure 4

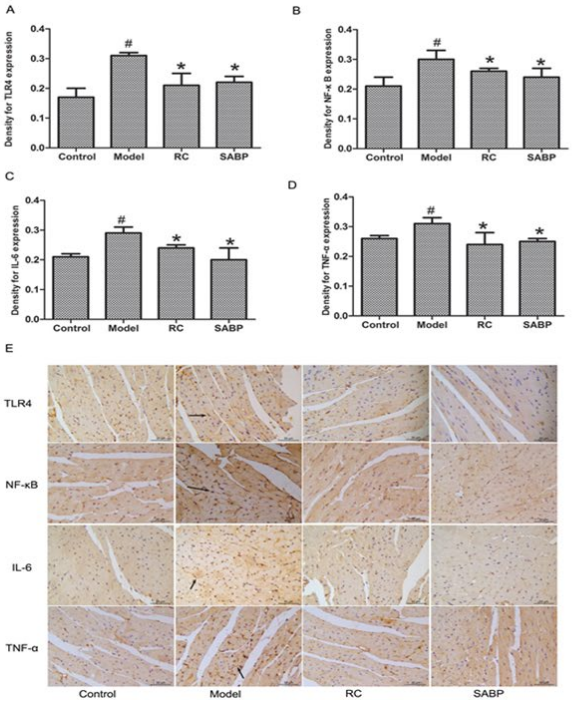
A
Density for TLR4 expression
0.0
0.1
0.2
0.3
0.4
#
*
*
Control
Model
RC
SABP
B
Density for NF-κ B expression
C
Density for IL-6 expression
D
Density for TNF-α expression
E
TLR4
NF-κB
IL-6
TNF-α
Control
Model
RC
SABP

Figure 5

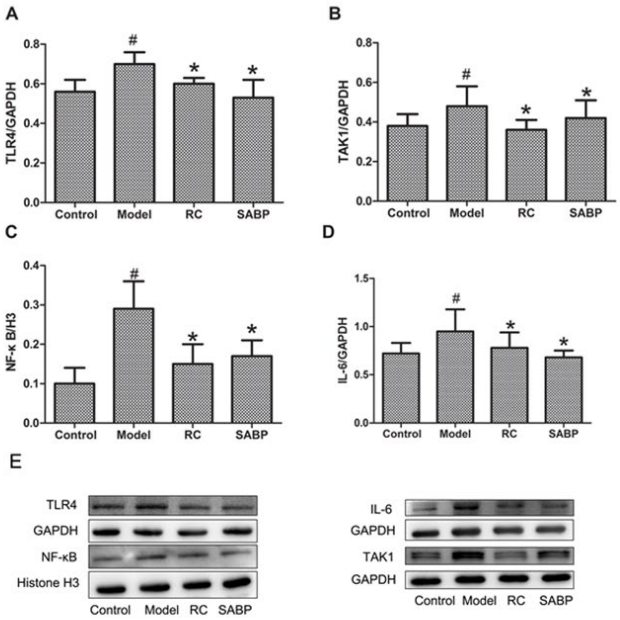
A
TLR4/GAPDH
0.0
0.2
0.4
0.6
0.8
#
*
*
Control
Model
RC
SABP
B
TAK1/GAPDH
0.0
0.2
0.4
0.6
0.8
#
*
*
Control
Model
RC
SABP
C
NF-κ B/H3
0.0
0.1
0.2
0.3
0.4
#
*
*
Control
Model
RC
SABP
D
IL-6/GAPDH
0.0
0.5
1.0
1.5
#
*
*
Control
Model
RC
SABP
E
TLR4
GAPDH
NF-κB
Histone H3
Control
Model
RC
SABP
IL-6
GAPDH
TAK1
GAPDH
Control
Model
RC
SABP

gure 6

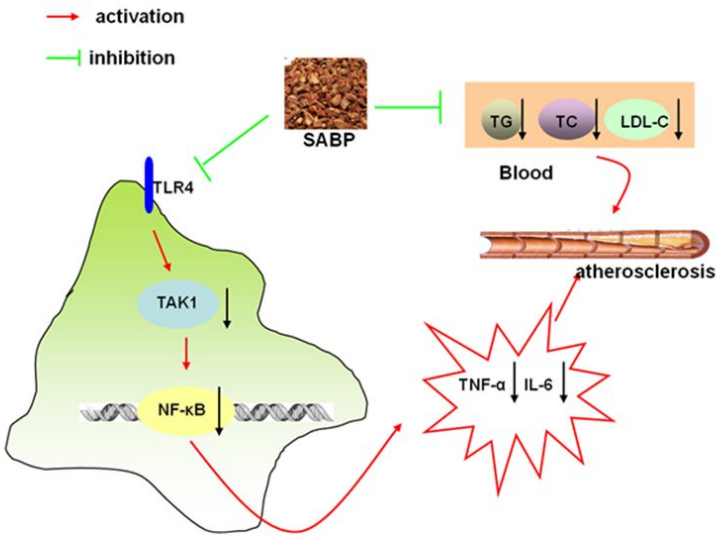
activation
inhibition
SABP
TG
TC
LDL-C
Blood
TLR4
atherosclerosis
TAK1
NF-κB
TNF-α
IL-6

Figure 7

Figures

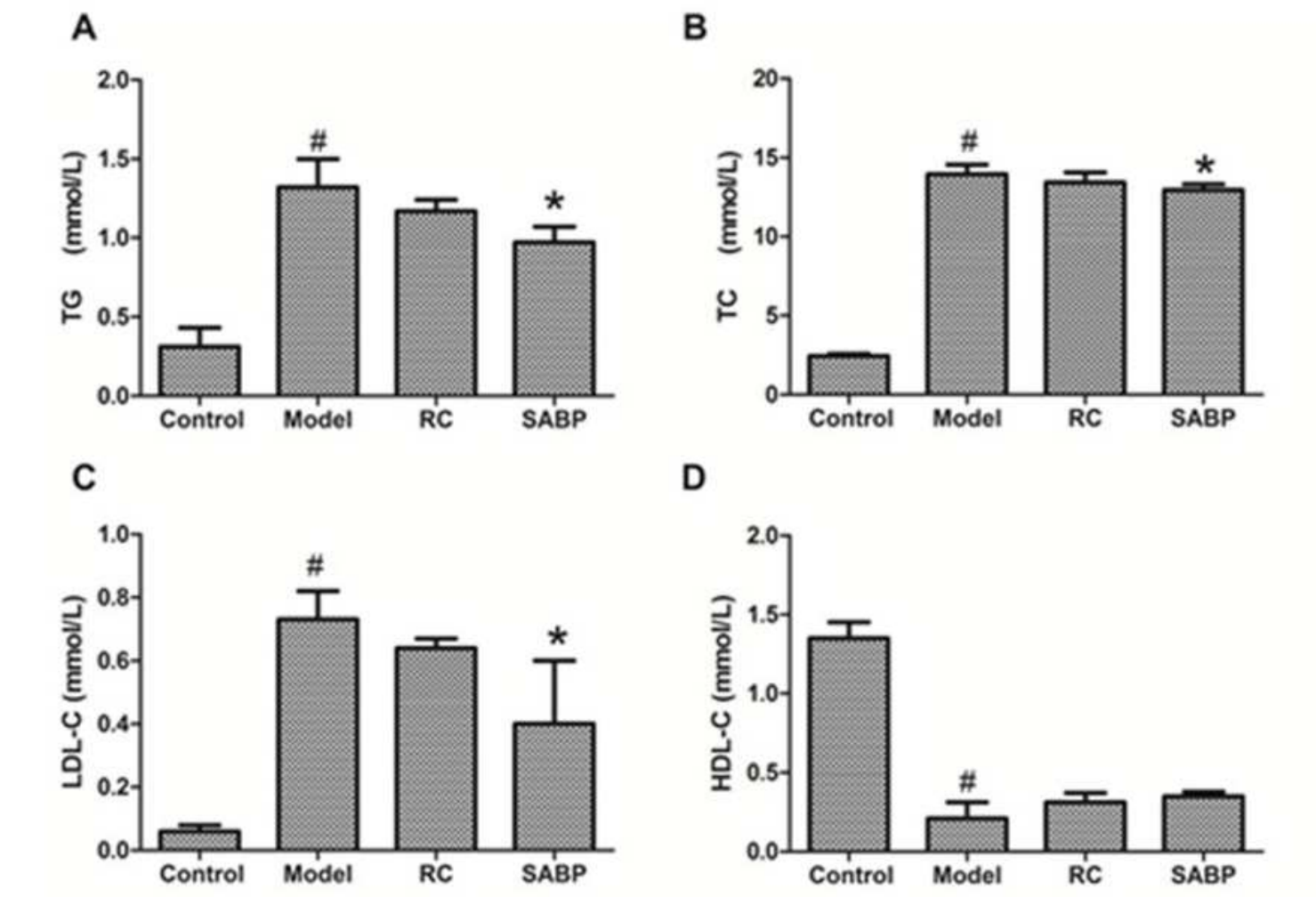

Figure 1

TG, TC, LDL-C, and HDL-C serum lipid levels in response to SABP treatment. (A) The TG level; (B) The TC level; (C) The LDL-C level; (D) The HDL-C level. Data are presented as mean ± SEM. n=6 in each group. # P<0.05, compared with the control group; *P<0.05, compared with the model group.

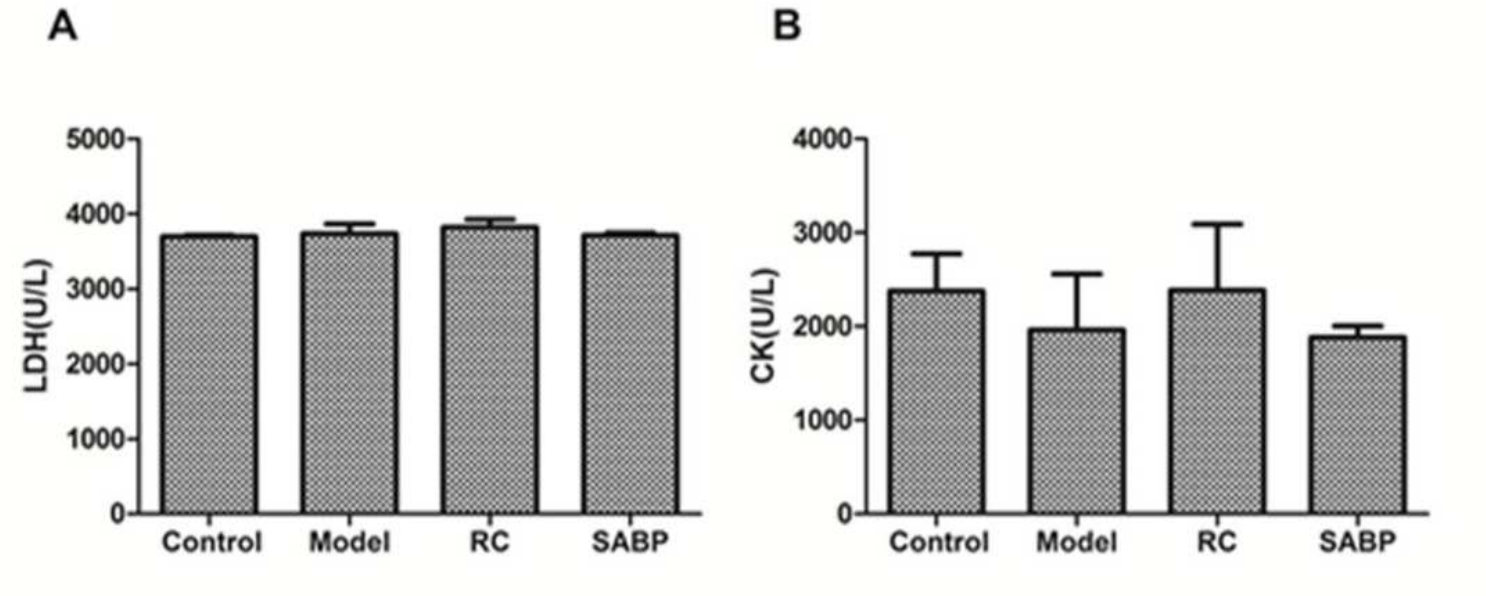

Figure 2

The LDH and CK levels in the heart in response to SABP treatment. (A) The LDH level in the heart; (B) The CK level in the heart. Data are presented as mean ± SEM. n=6 rats in each group.

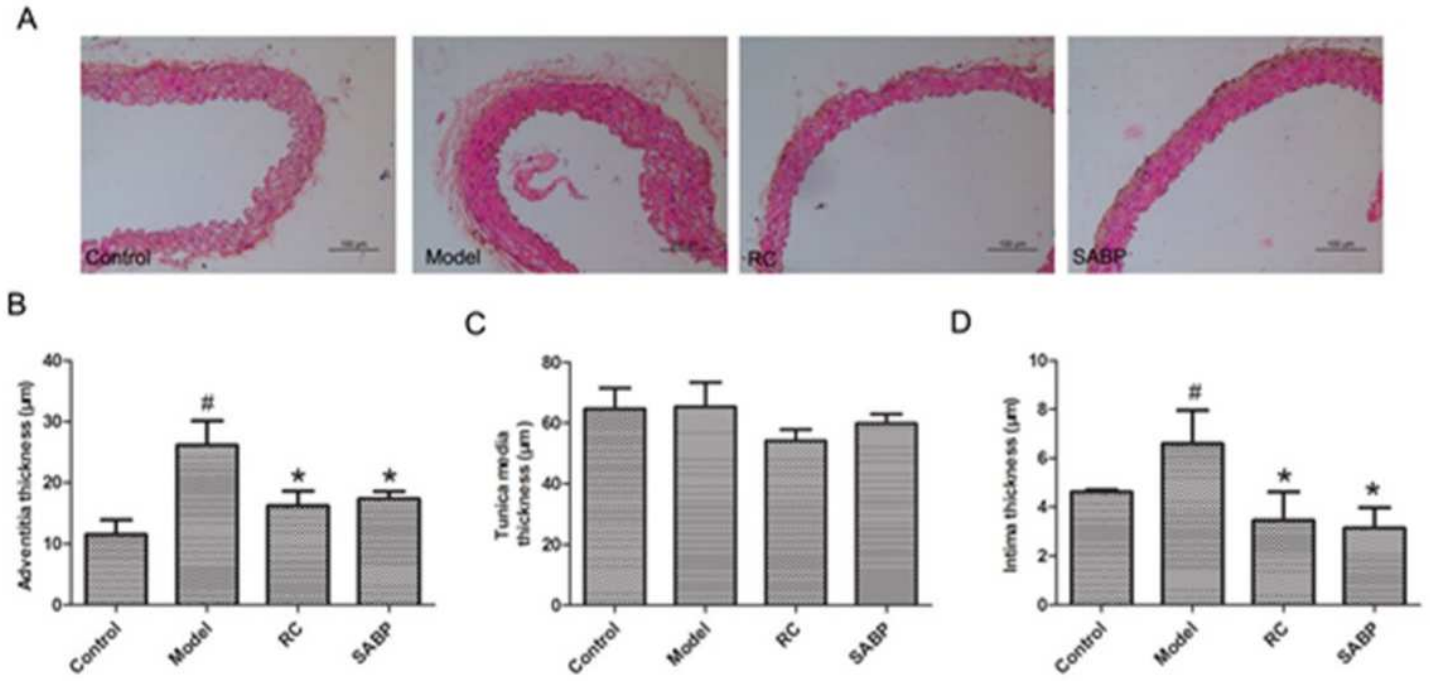

Figure 3

SABP attenuated the degree of AS-related lesion of the aorta in ApoE-/- mice. (A) HE staining of the aorta; (B) The adventitia thickness; (C) The tunica media thickness; (D) The intima thickness. Data are presented as mean ± SEM. n=6. #P<0.05, compared with the control group;*P<0.05, compared with the model group.

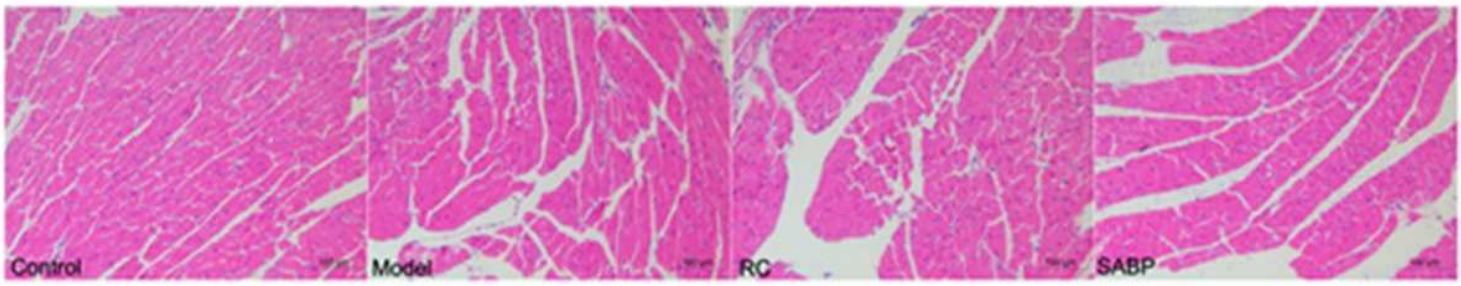

Figure 4

Observation of histologic changes of heart by HE staining.

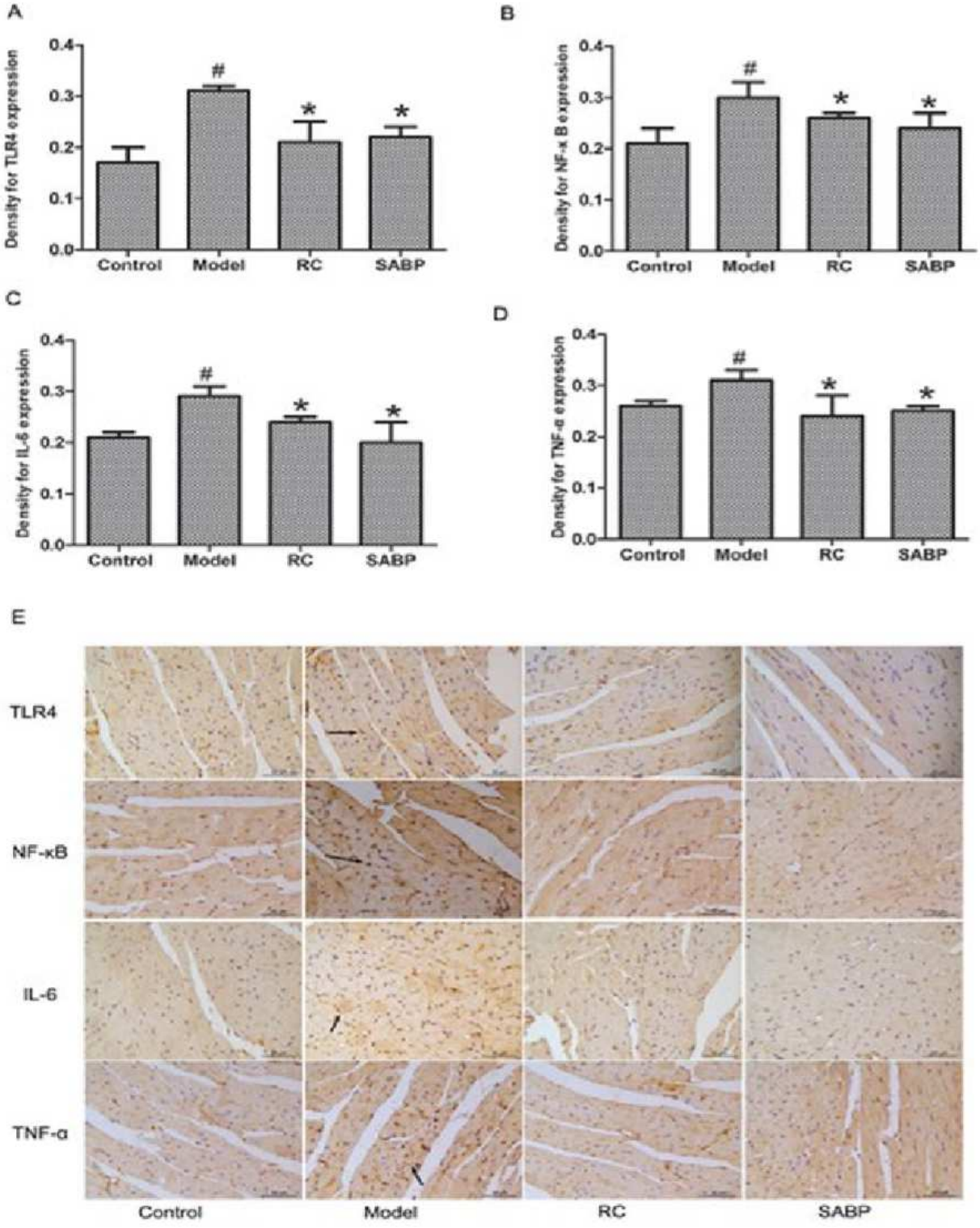

Figure 5

SABP suppressed TLR4, NF-κB, IL-6, and TNF-α expression in the heart. (A-D) Normalized quantitative data for TLR4, NF-κB, IL-6, and TNF-α protein expression levels; (E) The TLR4, NF-κB, IL-6, and TNF-α expression were displayed by immunohistochemistry staining. The arrows showed the staining for targeted protein. Values are expressed as mean ± SEM, n=4. #P<0.05, compared with the control group; *P<0.05, compared with the model group.

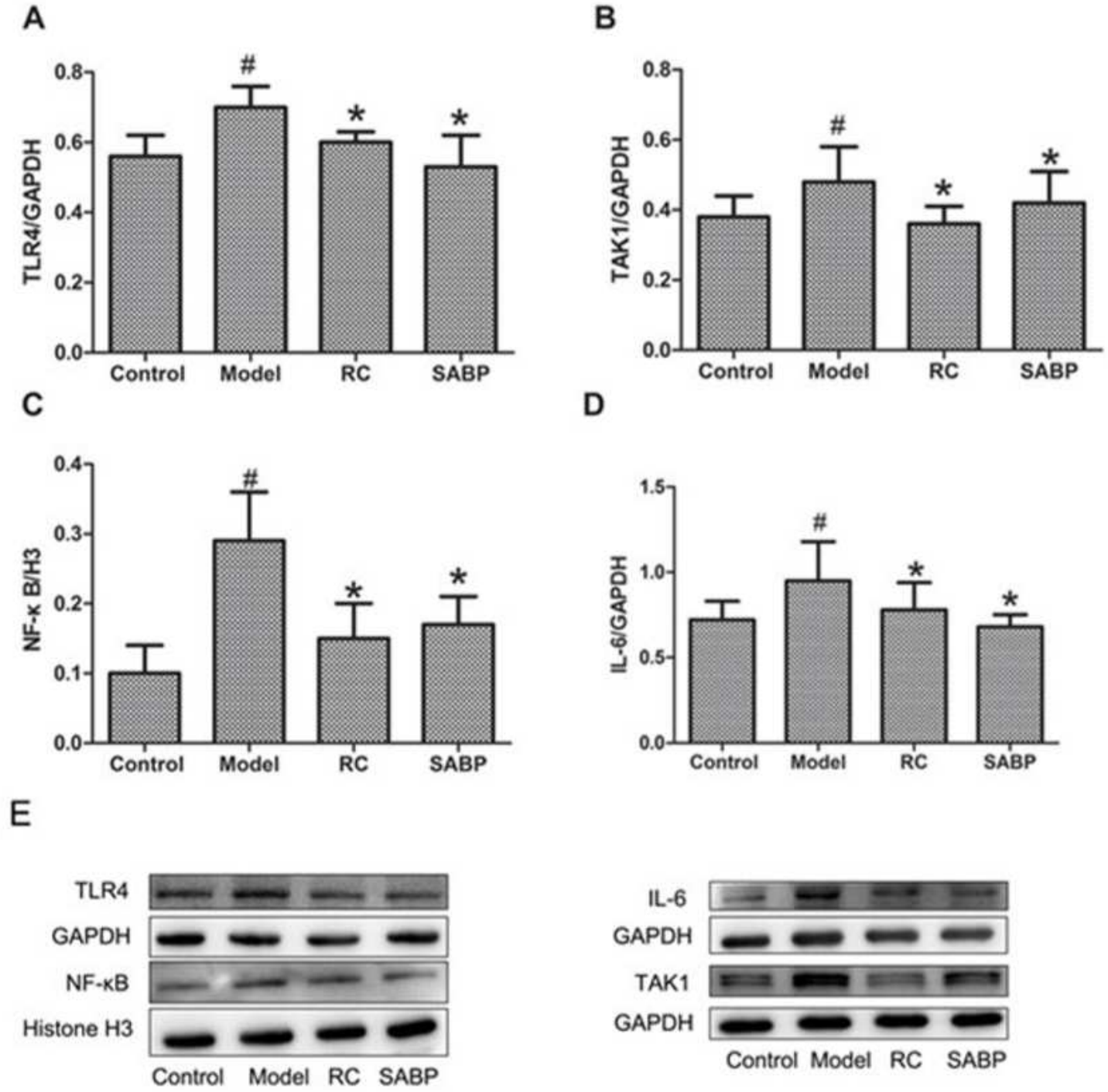

Figure 6

SABP treatment regulated the TLR4, NF-κB, IL-6, and TAK1 expression in the heart. (A-D) Normalized quantitative data for TLR4, NF-κB, IL-6, and TAK1 protein expression. (E-F) Western blotting bands showed the TLR4, NF-κB, IL-6, and TAK1 protein expression levels. GAPDH was used as an internal control for normalization. Values are expressed as mean ± SEM, n=4. #P<0.05, compared with the control group; *P<0.05, compared with the model group.

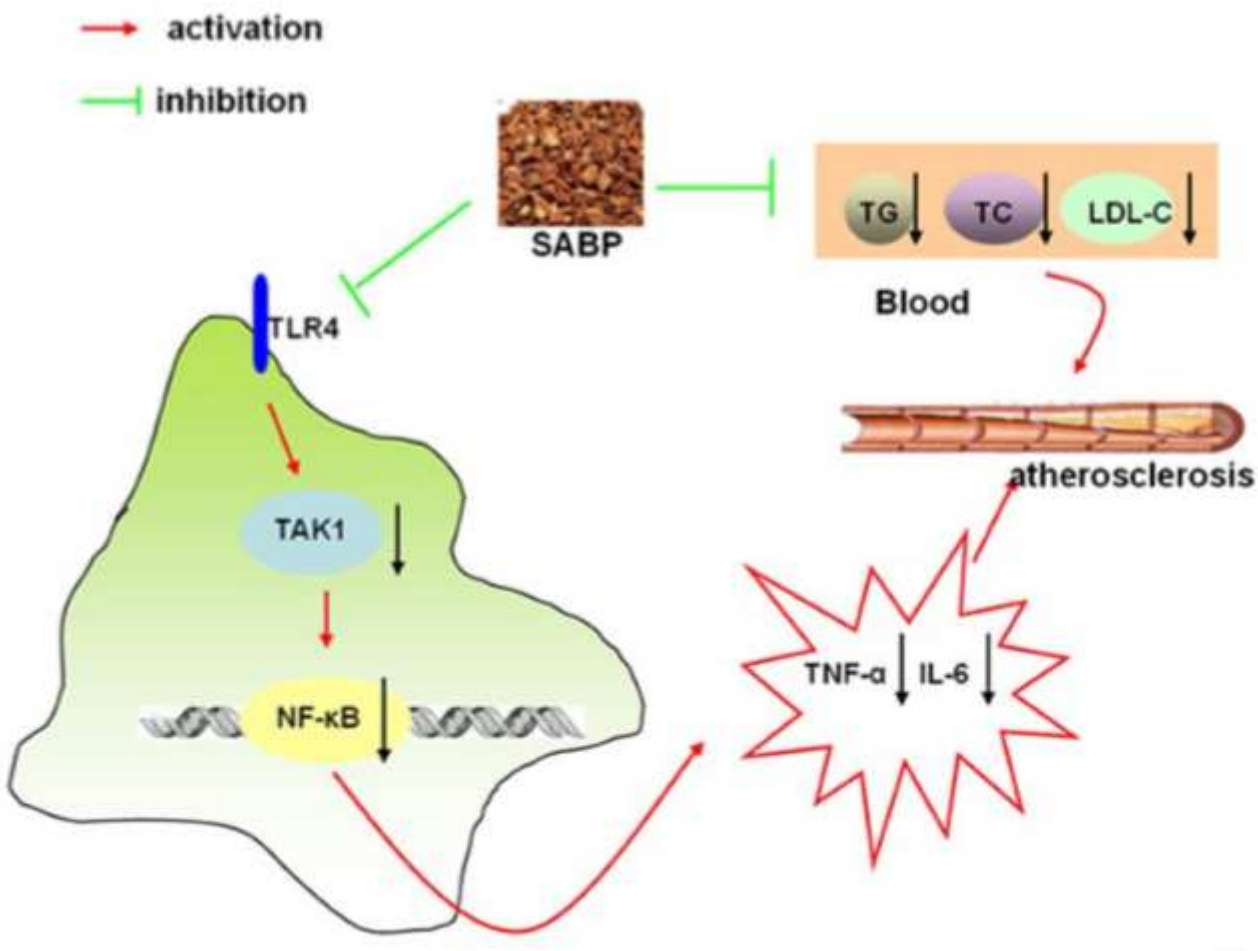

Figure 7

Compared with ApoE-/- mice in the model group, TLR4, TAK1, IL-6, and TNF-α protein were significantly decreased, and activated NF-κB was inhibited in SABP group ($P < 0.05$). These data indicated that SABP treatment regulated the AS by affecting the TLR4/NF-κB pathway and associated proteins.